

# Dielectric Polymers Tolerant to Electric Field and Temperature Extremes: Integration of Phenomenology, Informatics, and Experimental Validation

Chao Wu,<sup>†</sup> Lihua Chen,<sup>†</sup> Ajinkya Deshmukh, Deepak Kamal, Zongze Li, Pranav Shetty, Jierui Zhou, Harikrishna Sahu, Huan Tran, Gregory Sotzing, Rampi Ramprasad,<sup>\*</sup> and Yang Cao<sup>\*</sup>



Cite This: <https://doi.org/10.1021/acsami.1c11885>



Read Online

ACCESS |



Metrics & More



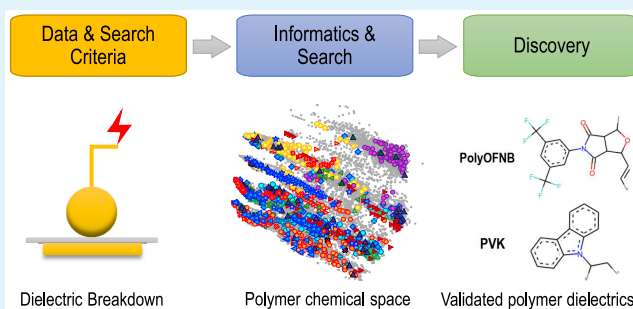
Article Recommendations



Supporting Information

**ABSTRACT:** Flexible polymer dielectrics tolerant to electric field and temperature extremes are urgently needed for a spectrum of electrical and electronic applications. Given the complexity of the dielectric breakdown mechanism and the vast chemical space of polymers, the discovery of suitable candidates is nontrivial. We have laid the foundation for a systematic search of the polymer chemical space, which starts with “gold-standard” experimental measurements and data on the temperature-dependent breakdown strength ( $E_{bd}$ ) for a benchmark set of commercial dielectric polymer films. Phenomenological guidelines are derived from this data set on easily accessible properties (or “proxies”) that are correlated with  $E_{bd}$ . Screening criteria based on these proxy properties (e.g., band gap, charge injection barrier, and cohesive energy density) and other necessary characteristics (e.g., a high glass transition temperature to maintain the thermal stability and a high dielectric constant for high energy density) were then setup. These criteria, along with machine learning models of these properties, were used to screen polymers candidates from a candidate list of more than 13 000 previously synthesized polymers, followed by experimental validation of some of the screened candidates. These efforts have led to the creation of a consistent and high-quality data set of temperature-dependent  $E_{bd}$ , and the identification of screening criteria, chemical design rules, and a list of optimal polymer candidates for high-temperature and high-energy-density capacitor applications, thus demonstrating the power of an integrated and informatics-based philosophy for rational materials design.

**KEYWORDS:** energy storage, dielectric polymers, breakdown, informatics, machine learning



## INTRODUCTION

Polymer dielectrics are key components of integrated electronic and electrical systems for insulating, power conversion and energy storages.<sup>1–3</sup> The miniaturization of electronic devices requires thin-film dielectrics that can endure higher electric fields. Additionally, there is an increasing need for high-energy-density polymer dielectrics for applications with the ultrahigh power density and operating under elevated temperatures, e.g., electrification in transport systems, aerospace, drilling, and gas explorations.<sup>3,4</sup> Given the practical and technological significance, it is desirable to discover polymers that are tolerant to an enormous electric field and high temperature for various applications.

In the past decades, extensive experimental and computational efforts have been spent to understand the polymer breakdown mechanisms and develop polymers with high breakdown strengths ( $E_{bd}$ ).<sup>4–8</sup> Although the influences of defects/interfaces,<sup>9,10</sup> cross-linking, molecular weight, and crystal structure<sup>11</sup> on breakdown have been extensively investigated, polymer breakdown mechanisms have not been

fully understood. Additionally, nanocomposites or surface coating techniques (involving large-band-gap inorganic materials such as  $\text{SiO}_2$ ,  $\text{Al}_2\text{O}_3$ , and  $\text{BN}^{4,5}$ ) have been proposed to suppress the charge injection and charge transport. Nevertheless, the performance (such as  $E_{bd}$ ) of these nanocomposites is still constrained by the all-organic polymer matrix and there are limitations to these approaches for scale-up. The discovery of all-organic polymers with high  $E_{bd}$  continues to be an important research and technological frontier. Identifying key factors that control  $E_{bd}$  is critical to this quest.

Through intensive research, a polymer dielectric codesign platform, involving the high-throughput computational model-

**Special Issue:** Artificial Intelligence/Machine Learning for Design and Development of Applied Materials

**Received:** June 24, 2021

**Accepted:** August 13, 2021

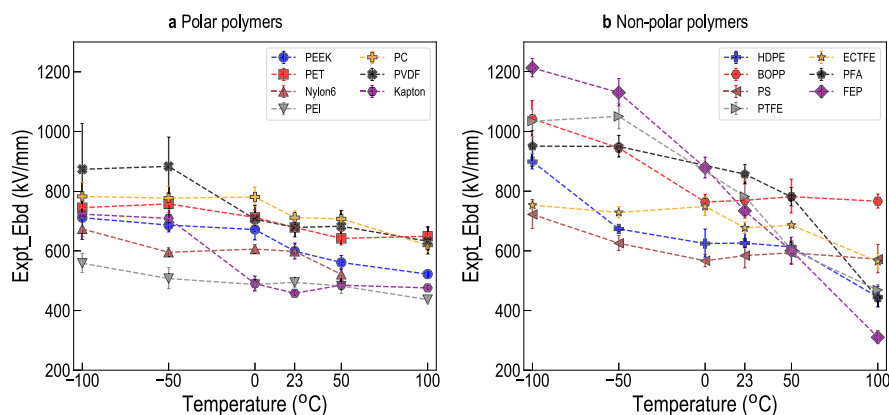


**Figure 1.** Temperature-dependent breakdown strength ( $E_{bd}$ ) of 14 commercial polymer film dielectrics: (a) polar and (b) nonpolar polymers. Error bars denote the 90% confidence interval of the Weibull distribution.

ing scheme and chemical synthesis and electrical characterization screenings, has been developed and led to plenty of polymers studied computationally and experimentally.<sup>6,12</sup> The most promising polymers (including both organic and organometallic polymers) possess a combination of high  $E_{bd}$ , large dielectric constant, low loss, and high energy storage capacity.<sup>6,12,13</sup> Additionally, several families of organic polythiureas, ureas, and imides were developed, on the basis of a design methodology for high-energy-density polymers with enhanced dipolar and ionic polarization that was revealed through extensive dielectric polarization mapping and high field characterization.<sup>12,13</sup> However, a refined codesign strategy is needed for the discovery of polymer dielectrics with not only high energy density but also high temperature withstanding capability.

In this work, an informatics-experiment-based approach was developed to accelerate the design of polymer dielectrics tolerant to enormous electric field and temperature. In this approach, first, comprehensive temperature-dependent breakdown experiments were performed to provide high-quality  $E_{bd}$  data for extensive statistical analysis, see Figure 1. Second, correlations between 10 electronic, thermal, and mechanical properties and  $E_{bd}$  were investigated. Results in Figure 2 illustrate that the band gap ( $E_g$ ) and the electron injection barrier for the aluminum electrode ( $\phi_e^{Al}$ ) exhibit strong positive correlations with  $E_{bd}$  at  $-100$  °C, whereas the cohesive energy density (CED) negatively impacts  $E_{bd}$ . As a result, these three properties were selected to screen polymers with high  $E_{bd}$ . Further, glass transition temperature ( $T_g$ ) and dielectric constant at 100 Hz ( $\epsilon_{100\text{ Hz}}$ ) were used as proxies of thermal stability and dielectric polarization, respectively. Third, these five proxies (i.e.,  $E_g$ ,  $\phi_e^{Al}$ , CED,  $\epsilon_{100\text{ Hz}}$ , and  $T_g$ ) of 13 000 all-organic polymers were predicted using previously developed machine learning models,<sup>14,15</sup> followed by the down-selection procedure with proposed screening criteria (Figure 3). Finally, we proposed nine representative polymers satisfying property requirements and synthesis feasibility. Two of nine polymers were lab synthesized for validation, showing exceptional properties. Furthermore, chemical design rules were proposed for high-energy-density polymers tolerant to extreme temperature, providing a pathway for the rational design of polymer dielectrics. Given the vast polymer chemical space, we believe that the developed approach can be effective in the discovery and design of polymers tolerant to enormous electric field and temperature.

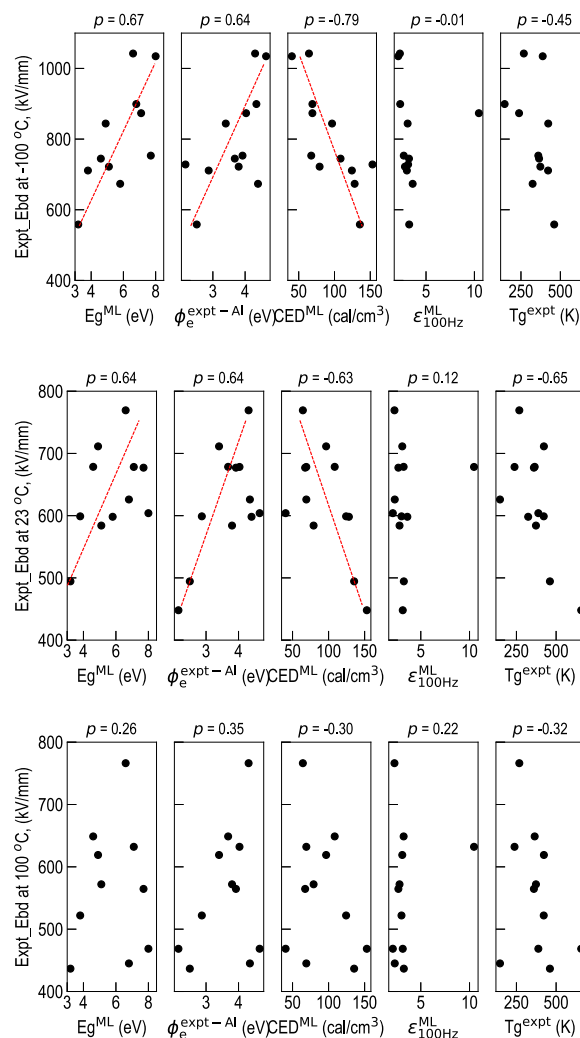


**Figure 2.** Correlation between  $E_{bd}$  at  $-100$ ,  $23$ , and  $100$  °C and five key proxies, including ML predicted band gap ( $E_g^{ML}$ ), experimental electron charge injection barriers for the aluminum electrode ( $\phi_e^{expt-Al}$ ),<sup>9</sup> ML predicted cohesive energy density (CED<sup>ML</sup>), ML predicted dielectric constant at 100 Hz ( $\epsilon_{100\text{ Hz}}^{ML}$ ), and experimental glass transition temperature ( $T_g^{expt}$ ).<sup>16</sup>

## EXPERIMENTAL SECTION

**Breakdown Tests.** The measurement is based on a Delta 9023 automated environmental chamber so that the  $E_{bd}$  of polymer films

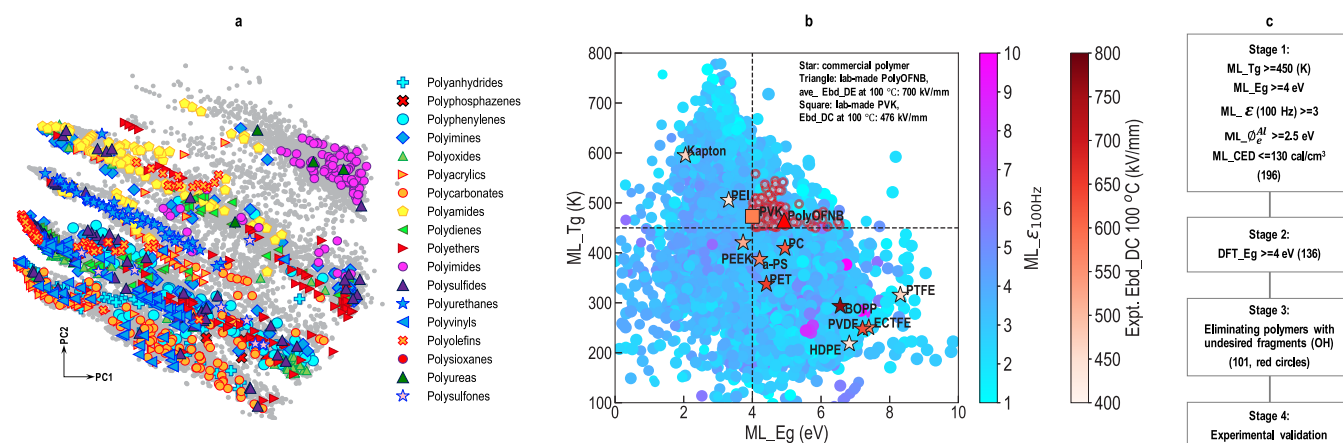


**Figure 3.** (a) Chemical space of 13 000 previously synthesized polymers, illustrated using the first two principle components (PC1 and PC2). (b) Property heatmap of ML  $T_g$ , ML  $E_g$ , ML  $\epsilon_{100 Hz}$ , and ML  $\phi_e^{Al}$  (circles size) of 13 000 polymers. The ML CED values are shown in Figure S3. Expt.  $E_{bd}$  DC values at 100 °C of 11 commercial polymers (stars) and lab-made PVK (square) and the average  $D-E$  loop  $E_{bd}$  of PolyOFNB (triangle) are provided. (c) Down-selection procedure for polymer dielectrics screening.

over a broad range of temperatures from cryogenic to elevated temperatures can be conducted.  $E_{bd}$  is measured using ball-plate electrodes with a fixed 300 V/s voltage ramp until breakdown, and the maximum voltage is recorded with a voltmeter. A special sample holder was built to load up to ten sample sets for every test run (Figure S1). Each sample has a separate high-voltage feed-through over the oven wall. All samples are tested with multiple specimen at every specific temperature point to generate ten breakdown data points for Weibull statistical analysis:  $P(E_{bd}) = 1 - \exp[-(E_{bd}/\alpha)^\beta]$ , where  $P(E_{bd})$  is the cumulative probability of failure,  $E_{bd}$  is the breakdown strength,  $\alpha$  is the evaluated breakdown strength in Figure 1 that denotes a 63.2% probability to breakdown, and  $\beta$  is the shape parameter that represents the dispersion of breakdown data.

**Machine Learning.** Machine learning models for  $T_g$ ,  $\epsilon$ , CED,  $E_g$ , and  $\phi_e^{Al}$  prediction of polymers were developed in our previous work, using hierarchical polymer fingerprints and Gaussian process regression.<sup>14,15</sup>  $T_g$ ,  $\epsilon$ , and CED were trained using experimental values, whereas  $E_g$  and  $\phi_e^{Al}$  were trained using DFT computed values of single-chain polymers. The details are addressed in refs 14 and 15 and all models are implemented in the *Polymer Genome* platform (<https://www.polymergenome.org>). Additionally, the 13 000 synthesized polymers in Figure 3 were manually collected from the literature, polymer handbook,<sup>16</sup> and online repositories.<sup>17</sup> They are composed of 12 elements, including C, H, O, N, S, P, B, Cl, F, Br, I, and Si, and various polymer classes, such as polyimides, polyamide, polyolefins, and polyfulones. To visualize the chemical diversity of these 13 000 polymers, we analyzed their chemical features using PCA, as shown in Figure 3a.

**Density Functional Theory Computations.** The single-chain structures of 160 polymers in stage 2 of Figure 3b were generated using the polymer structure predictor (PSP).<sup>18</sup> The relaxed structures were further used to compute  $E_g$  using hybrid DFT, as implemented in VASP.

## RESULTS AND DISCUSSION

**Temperature-Dependent Breakdown Strength.** The breakdown process of dielectric materials is intriguing and complicated because of the interplay of multiple temperature-dependent electronic, thermal, and mechanical factors. High-fidelity breakdown strength data thus form the basis of targeted searches for polymers with high field withstanding capability because the breakdown strength cannot be computed through first principles. The temperature dependence of dielectric breakdown has long been observed;<sup>19</sup> however, up until now, only limited systematic studies have been conducted on such temperature dependence, especially for polymer thin films.

With the availability of polymers processed with modern film-forming methods, i.e., biaxial orientation, there is a great need to revisit and update those basic investigations by considering various characteristics of polymer dielectrics, e.g., polarity (polar and nonpolar), morphology (semicrystal and amorphous), and monomer chemistry (aliphatic and aromatic). Fourteen commercial polymer film dielectrics were selected for experimental investigation in this study to minimize the introduction of defects during small-scale laboratory synthesis to ensure the reliability of the experimental data of breakdown strength (Table S1). Figure 1 illustrates the temperature-dependent  $E_{bd}$  of seven polar polymers and seven nonpolar polymers, ranging from  $-100$  to  $100$  °C. We note that the 14 polymer films investigated here have high  $E_{bd}$  values, ranging from 300 to 1200 kV/mm. The measured  $E_{bd}$  values of BOPP, as the state-of-the-art capacitive dielectric, are 1050 kV/mm at  $-100$  °C and 800 kV/mm at room temperature. It is also worth mentioning that FEP has the maximum  $E_{bd}$  of about 1200 kV/mm at  $-100$  °C, whereas its  $E_{bd}$  value dramatically drops to the lowest (300 kV/mm) as the temperature increases to 100 °C. For high-temperature applications, the lower temperature dependence of breakdown strength is as significant as intrinsically high breakdown strength.

As shown in Figure 1,  $E_{bd}$  of these 14 polymers generally decreases with an increase in the temperature. The temperature dependence of polymers with nonpolar structure is more than that of polar polymers overall, although exceptions like nonpolar PS and ECTFE also revealed relatively lower temperature dependence. In specific temperature ranges,  $E_{bd}$  for most of the nonpolar polymers, i.e., BOPP, FEP, HDPE, PTFE, and PFA, decreased dramatically, with varying degrees among these polymers. These five polymers are aliphatic and have relatively low  $T_g$ , the highest of which is only 106 °C for PTFE. Approaching or exceeding  $T_g$ , the large scale of segmental motions gives rise to high polarization loss and poor mechanical strength, which might induce the dramatic drop of  $E_{bd}$  observed.  $T_g$  is the upper operational temperature limit for polymers with amorphous structure because of the diminished mechanical strength above  $T_g$ . Although semicrystalline polymers (like BOPP, HDPE, and PTFE) can operate at temperatures ranging from  $T_g$  to the melting temperature, the significant drop of  $E_{bd}$  above the glass

transition indicates that  $T_g$  is a vital parameter even for semicrystalline polymers. Except for Nylon-6, polar polymers studied all have aromatic structures, contributing to better thermal stability. Thermally stable polymers, such as Kapton, PEI, PEEK, and PC with high  $T_g > 150$  °C, exhibit relatively stable  $E_{bd}$  in the temperature range investigated compared to those nonpolar polymers with low  $T_g$ . These findings indicate the significant impact of  $T_g$  on the temperature dependence of  $E_{bd}$ .

**Correlation Analysis between Breakdown Strength and Key Factors.** Key proxies arising from electronic, thermal, and mechanical properties affecting  $E_{bd}$  should be identified to turn the empirical qualitative observations into accurate design rules to power the targeted discovery of polymer dielectrics.<sup>19</sup> The correlations between  $E_{bd}$  at  $-100$ ,  $23$ , and  $100$  °C of 12 homopolymers in Figure 1 (excluding copolymers PFA and FEP) and 10 proxy properties have been studied using Pearson correlation analysis. Pearson coefficient ( $p$ ) approaching 1 ( $-1$ ) represents a strong positive (negative) correlation. Figure 2 illustrates five proxy properties, including  $E_g$ , CED,  $\epsilon_{100\text{ Hz}}$ ,  $\phi_e^{\text{Al}}$ , and  $T_g$ . Another five properties are displayed in Figure S2, i.e., density ( $\rho$ ), thermal conductivity ( $\kappa$ ), heat capacity ( $C_p$ ), Young's modulus (YM), and tensile strength (TS). Furthermore,  $E_g$ , CED, and  $\epsilon_{100\text{ Hz}}$  are machine learning (ML) predicted values using our previously developed models.<sup>14,15</sup> In terms of the remaining seven properties, we used room-temperature measured values because of the limited availability of temperature-dependent data. Additionally, morphology (amorphous and semicrystalline) plays a critical role in determining the breakdown of polymers; however, given that morphology depends on the processing conditions, this factor is not considered in this work.

From Figure 2, we note that  $E_{bd}$  at  $-100$  and  $23$  °C is positively correlated with  $E_g$  and  $\phi_e^{\text{Al}}$ , with  $p > 0.64$ .  $E_g$  is the energy gap between the valence band and conduction band, i.e., the excitation energy of electrons from the valence band to the conduction band.  $\phi_e^{\text{Al}}$  is the energy barrier for electron injection from electrodes into polymer films.<sup>20,21</sup> Therefore, both high  $E_g$  and  $\phi_e^{\text{Al}}$  lead to low concentration and energy of free electrons within polymers and thus high  $E_{bd}$ . Further, the thermal motion and deformation of polymer chains is constrained in the low temperature, so that  $E_{bd}$  is dominated by the electronic properties of the polymer bulk and its interface with electrodes. It is also interesting to observe that  $E_{bd}$  at  $-100$  and  $23$  °C of these 12 polymers depends negatively on CED, with a  $p$  value of  $-0.79$  and  $-0.63$ , respectively, indicating a possible negative correlation between  $E_g$  and CED, as shown in Figure S3. Higher CED is derived from strong interchain interactions, such as hydrogen-bonding and van der Waals forces, degrading the overlaps of antibonding energy levels of polymers and thus decreasing  $E_g$ . This finding is different from the past study, which shows a positive correlation of  $E_{bd}$  and CED based on data obtained at higher temperatures.<sup>19</sup> This might imply the dominant role of temperature in determining the crystalline structures of polymers and hence their electronic properties that affect  $E_{bd}$ , which is considered more intrinsic toward cryogenic temperatures.

In contrast, these correlations between  $E_{bd}$  and  $E_g$ ,  $\phi_e^{\text{Al}}$ , and CED are weaker at  $100$  °C, because of a significant drop in  $E_{bd}$  for HDPE and PTFE at  $100$  °C. In the high temperature range, thermal and mechanical factors contribute more to the breakdown of polymers, especially for polymers with relatively

low  $T_g$ . In general,  $100$  °C is well above (for HDPE) or approaching (for PTFE) their  $T_g$ . The increasing thermal motion of polymer chains and compromised mechanical strength resulted in reduced  $E_{bd}$  of HDPE and PTFE at  $100$  °C. Decoupled more from the impact of thermal and mechanical factors,  $E_{bd}$  at a cryogenic temperature of  $-100$  °C can be better correlated to (intrinsic) electronic parameters. Therefore, electronic parameters of  $E_g$ ,  $\phi_e^{\text{Al}}$ , and CED (negatively) correlated highly to  $E_{bd}$  at  $-100$  °C can be utilized as key proxies in a more targeted searches of polymers with intrinsically high  $E_{bd}$ .

For electronic and electrical applications, polymer dielectrics with desired  $\epsilon$  values are also requested to achieve high energy density.<sup>13,22,23</sup> Figure 2 reveals that there is no clear correlation between  $E_{bd}$  and  $\epsilon_{100\text{ Hz}}$  at  $-100$ ,  $23$ , and  $100$  °C for 12 polymers investigated. However, it is worth mentioning that there is a strong negative correlation between  $\epsilon_{100\text{ Hz}}$  and  $E_{bd}$  for other polymers, if excluding high polar PVDF (ML predicted  $\epsilon_{100\text{ Hz}} = 10.45$ ). This is mainly because the electronic part of  $\epsilon$  exhibits an inverse relationship with  $E_g$  and thus  $E_{bd}$ .<sup>6</sup>

The fifth proxy,  $T_g$ , is a measure of the thermal stability of polymers and a critical design parameter for applications under harsh conditions (elevated temperatures).<sup>3,4</sup> We found that  $E_{bd}$  is slightly and negatively correlated with  $T_g$ , with a  $p$  of  $-0.45$ ,  $-0.65$ , and  $-0.32$  at  $-100$ ,  $23$ , and  $100$  °C, respectively. One of the reasons is that higher  $T_g$  can degrade  $E_g$  of polymers, because of the introduction of many unsaturated aromatic rings. This is supported by the fact that a majority of thermally stable polymers have moderate  $E_{bd}$  values, such as PEI and Kapton in Figure 1. However, higher  $T_g$  is desired for better thermal stability, as well as less temperature dependence for  $E_{bd}$ .

Additionally, Figure S2 reveals that  $E_{bd}$  at all temperatures is not well correlated with the remaining five properties including  $\rho$ ,  $\kappa$ ,  $C_p$ , TS, and YM. A plausible explanation is that  $\kappa$  and  $C_p$  play a more important role only in the thermal breakdown mechanism, whereas the mechanical properties are more correlated to electromechanical breakdown of polymers. The thermal and mechanical properties may contribute more to the temperature dependence of  $E_{bd}$ .

#### Machine-Learning-Aided Polymer Dielectrics Design.

Not only can the key proxies discussed above help to provide insights into the breakdown mechanisms but they also serve as screening criteria for accelerated targeted search of desired polymer dielectrics from an enumerated candidate pool.<sup>12,14,15,22,24–28</sup> To achieve this goal, ML prediction models are utilized to predict the required proxies of the enumerated candidate polymers for the target application. It is followed by a down-selection procedure based on the screening criteria, resulting in optimal candidates for experimental validation.

As illustrated in Figure 3a, about 13 000 previously synthesized polymers have been manually accumulated from various resources, such as polymer handbooks and repositories.<sup>15–17,29,30</sup> These polymers are made up of 12 elements, i.e., C, H, B, O, N, S, P, Si, F, Cl, Br, and I, into various classes, e.g., polyolefins, polyimides, polyvinyls, polyethers, polyesters, polydienes, polyoxides, and polycarbonates. The chemical space is illustrated in Figure 3a using the first two (PC1 and PC2) components obtained from the principal component analysis (PCA) on the chemical features of 13 000 polymers. To be good candidates for high-temperature, high-energy-

density capacitors, polymers need high  $E_{bd}$ , energy density and good thermal stability at high temperature window. According to the correlation analysis in Figure 2, large  $E_g$ , high  $\phi_e^{Al}$ , and low CED lead to high  $E_{bd}$ . Further, high  $T_g$  is desired to sustain the thermal stability in an extremely high temperature window and high  $\epsilon$  is required to obtain a high energy density. Therefore, these five proxy properties were selected to screen candidates from 13 000 polymers for high-temperature and high-energy-density capacitors, as summarized in Table 1.

**Table 1. Screening Criteria for Polymer Dielectrics Tolerant to Enormous Electric Fields and Temperature<sup>a</sup>**

proxy	desired values	comments
$E_g$	$\geq 4$ eV	positive correlation with $E_{bd}$
$\phi_e^{Al}$	$\geq 2.5$ eV	positive correlation with $E_{bd}$
CED	$\leq 130$ cal/cm <sup>3</sup>	negative correlation with $E_{bd}$
$T_g$	$\geq 450$ K	maintaining good thermal stability in high temperature-window
$\epsilon_{100\text{ Hz}}$	$\geq 3$	achieving high energy density

<sup>a</sup>The desired values of  $E_g$ ,  $\phi_e^{Al}$  and CED are selected for  $E_{bd} \geq 500$  kV/mm at  $-100$  and  $23$  °C.

Figure 3b shows the ML predicted values of  $E_g$ ,  $T_g$ ,  $\epsilon_{100\text{ Hz}}$  and  $\phi_e^{Al}$  for 13 000 polymer candidates using our previously developed models.<sup>14,15</sup> The ML predicted CED is shown in Figure S3 of SI.  $E_{bd}$  values at 100 °C for 11 commercial polymers are overlaid in Figure 3b (denoted by stars) to show the performance of polymers in a high-temperature window. We note that there is an inverse relationship between  $T_g$  and  $E_g$ . As a result, polymers with very high  $T_g$  (e.g., PEI and Kapton) have low  $E_g$  (<4 eV) and thus medium  $E_{bd}$  (300–500 kV/mm). Although polymers with  $E_g$  ranging from 4 to 6 eV have high  $E_{bd}$  (>500 kV/mm), they have medium  $T_g$  and thus a medium temperature service window. When the  $E_g > 6$  eV, although  $E_{bd}$  values of BOPP, PVDF, and ECTFE are high (>500 kV/mm), HDPE and PTFE respectively drop to 445 and 468 kV/mm because of the low  $T_g$  and poorer thermal stability. Moreover, Figure 2 shows that  $\phi_e^{Al} \geq 2.5$  eV and CED  $\leq 130$  cal/cm<sup>3</sup> are required to reach high  $E_{bd} > 500$  kV/mm at  $-100$  and  $23$  °C (even for 100 °C). Consequently, criteria of  $E_g \geq 4$  eV,  $T_g \geq 450$  K, and  $\phi_e^{Al} \geq 2.5$  eV,  $\epsilon_{100\text{ Hz}} \geq 3$ , and CED  $\leq 130$  cal/cm<sup>3</sup> (see Table 1) were selected to screen polymer candidates for high-temperature, high-energy-density capacitors.

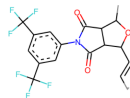
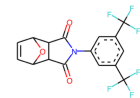
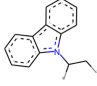
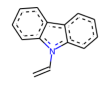
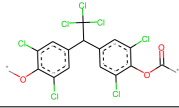
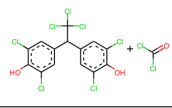
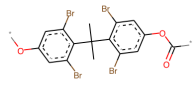
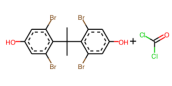
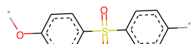
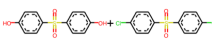
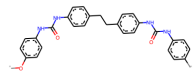
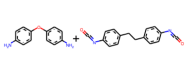
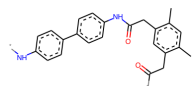
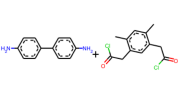
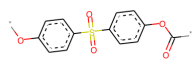
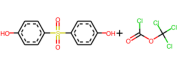
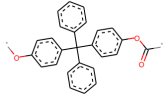
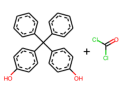
Next, we move on to down-select polymer candidates<sup>3,4,31,32</sup> using four stages, as illustrated in Figure 3c. In stage 1, ML predicted  $T_g \geq 450$  K,  $E_g \geq 4$  eV,  $\epsilon_{100\text{ Hz}} \geq 3$ ,  $\phi_e^{Al} \geq 2.5$  eV, and CED < 130 cal/cm<sup>3</sup> were utilized to select 196 candidates from 13 000 polymers. Given that  $E_{bd}$  has a highly positive correlation with  $E_g$ , in stage 2, single-chain structures for 160 polymers were successfully generated and used to compute  $E_g$  using density functional theory (DFT) to further improve the accuracy of the screening. As a result, 136 candidates with  $E_g \geq 4$  eV were identified. Furthermore, polymers with the undesired hydroxyl fragment (OH) were further eliminated, resulting in 101 candidates (denoted by red circles in Figure 3b). This is because the OH group leads to high dielectric polarization loss, high water absorption, and low solubility in solvents induced by the strong H-bonding. Figure 4 lists 9 of 101 promising and synthesis-friendly polymer candidates,

including their repeat units, predicted property values, and required reactants<sup>5,17,34–38</sup> for polymer synthesis.

**Experimental Validation.** Out of nine polymers in Figure 4, PolyOFNB was a recently developed polymer candidate for high-temperature capacitors reported in our previous work.<sup>3</sup> It has a  $T_g$  of 459 K,  $E_g$  of 4.9 eV, and  $\epsilon$  of 2.5, contributing to stably high energy density at ambient and elevated temperatures.<sup>3</sup> The average  $E_{bd}$  of PolyOFNB is above 700 MV/m at room temperature (RT) and 100 °C measured by a displacement–electric field ( $D$ – $E$ ) loop tester (see Figure 3). This performance is comparable with the  $E_{bd}$  value at RT of the best established polymer tolerant to extremely high electric fields, BOPP, under the same test condition.<sup>3</sup> PolyOFNB possesses the ever highest discharged energy density of 5.7 J/cm<sup>3</sup> at 150 °C in comparison with the best reported flexible polymers or polymer composites.<sup>3,11,33</sup> This benchmark example successfully approves the methodology and screening criteria employed in this work.

To further demonstrate the validity of the informatics-based approach, we fabricated another candidate, polyvinylcarbazole (PVK), in films with a thickness of around 10  $\mu$ m deposited on polished stainless steel shimstock substrates.  $E_{bd}$  of PVK was investigated at RT and 100 °C. The Weibull statistics plotted in Figure S4 summarize  $E_{bd}$  of 13 breakdown tests for the identification of the characteristic  $E_{bd}$  values at 63.2% ( $1-1/e$ ) probability of failure.  $E_{bd}$  of PVK can reach up to 565 kV/mm at RT and 476 kV/mm at 100 °C. The statistical  $E_{bd}$  values at the 63.2% probability of failure of the Weibull distribution are 482 and 383 MV/m at RT and 100 °C, respectively. The slopes of the fitting line indicate the Weibull shape factor ( $\beta$ ). The shape factors characterize the dispersion of  $E_{bd}$  data and reveal the reliability of the polymer dielectrics under extremely high electric fields. Further, the shape factors  $\beta$  of the Weibull distribution for  $E_{bd}$  of PVK (7.5 at RT and 5.6 at 100 °C) are much lower than that of commercial films (generally >10). For instance, the shape factors are 27.4 at RT and 35.7 at 100 °C for Kapton and 15.9 at RT and 20.3 at 100 °C for PEI, two of the well-established high-temperature polymers. These results suggest that  $E_{bd}$  of PVK is still limited by the uniformity and stability of laboratory-synthesized film in comparison to the large-scale roll-to-roll processed commercial films. Despite the large space for further improvement through enhanced film processing,  $E_{bd}$  of PVK is already higher than that of the established high-temperature dielectrics, PEI and Kapton, attributable to its larger  $E_g$  and higher  $\phi_e$ .

**Guidelines for Designing Polymers Dielectrics.** To unveil chemical rules for the rational design of polymer dielectrics, we analyzed the frequency of constituting fragments of the 101 desired polymer candidates screened from stage 4 in Figure 3 using BRICS, as implemented in RDKit.<sup>39</sup> Here, the 10 most common fragments present in 13 000 polymers were excluded, including C=O, NH, O, and aromatic rings. The remaining top 20 representative fragments for these 101 polymers are illustrated in Figure 5. We notice that most fragments include cyclic rings, enhancing  $T_g$  and providing better thermal stability. However, conjugated (or unsaturated) cyclic rings (e.g., fragment 1, 3–5) degrade  $E_g$  by introducing  $\pi$  bonding energy levels, which is the key proxy in determining  $E_{bd}$  (see Figure 2). This issue can be solved by introducing saturated rings (e.g., fragments 7, 11, 13, 15, 16, 18), leading to a large  $E_g$  and  $\phi_e^{Al}$  as well as a high  $T_g$ . Additionally, polar fragments with C–Cl (ID 6), C–Br (ID 4), O (ID 2, 18), and N (ID 2) contribute to high  $\epsilon$  by introducing high electronic

ID	Monomer	T <sub>g</sub> (K)	E <sub>g</sub> (eV)	ε <sub>100Hz</sub>	φ <sub>e</sub> <sup>AI</sup> (eV)	CED (cal/cm <sup>3</sup> )	E <sub>bd</sub> (kV/mm)	Reactants	Ref
1	PolyOFNB 	466	5.18	3.05	2.56	91.7	700 (D-E)		[3]
2	PVK 	476	4.04	3.02	3.09	125.6	476 (DC)		This work
3		542	4.9	3.3	3.4	92.3	-		[17]
4		528	4.6	3.2	3.4	96.2	-		[34]
5		505	4.3	3.7	3.1	114.6	-		[17]
6		502	4.3	4.5	3.6	117.4	-		[35]
7		500	4.1	3.9	3.5	111.6	-		[36]
8		491	4.6	3.4	3.2	113.4	-		[37]
9		481	4.7	3.4	3.6	86.3	-		[38]

**Figure 4.** Nine representative and synthesis-friendly polymer candidates for high-temperature and high-energy-density capacitors.  $E_g$  is DFT predicted values,  $E_{bd}$  is experimental results at 100 °C, and the others are ML predicted values. The required reactants to synthesize the specific polymer are also provided.<sup>3,17,34–38</sup>

polarization. These findings unravel that polymers with well-designed benzene rings, saturated cyclic rings, and polar groups are suitable for capacitors serving in high temperature and extreme electric field conditions. Further, this design principle is validated experimentally by the high  $E_{bd}$  of PolyOFNB<sup>3</sup> and relatively high  $E_{bd}$  of PVK polymers in Figure 3. PolyOFNB and PVK both have a benzene ring, saturated cyclic structure, and polar fragments. The optimized combination of these fragments contributed to their high  $E_{bd}$  at elevated temperatures.

## CONCLUSION AND OUTLOOK

In this work, a targeted informatics-based codesign has been proposed to rapidly discover and design novel polymers tailored to energy storage in the extreme electric field and temperature. To power this targeted codesign search, we measured the temperature-dependent breakdown strengths of 14 commercial polymers systematically to provide high-fidelity  $E_{bd}$  data. Such golden data were further used to identify the key proxies in determining  $E_{bd}$  through extensive statistical analysis. The extensive statistical analysis reveals that  $E_{bd}$  positively

depends on  $E_g$  and  $\phi_e^{AI}$  and is negatively correlated with CED. These findings lay a great foundation to the design of polymers with high  $E_{bd}$ . Accordingly, five proxies have been identified to screen potential polymer dielectrics for high-density energy storage under high electric fields and high temperatures, including large  $E_g$ , high  $\phi_e^{AI}$ , low CED, high  $\epsilon$ , and high  $T_g$ . One-hundred and one optimal polymers were down-selected from 13 000 previous synthesized polymers and utilized to identify chemical design rules. Moreover, according to empirical chemical design rules, nine representative polymers are illustrated in Figure 4 for experimental validation. In the end, this polymer exploration approach is successfully validated by a recently reported PolyOFNB and a newly lab-made PVK.

Overall, this targeted informatics-based codesign approach possesses unique advantages. First, it can instantly provide predicted properties using the developed ML models (as implemented in Polymer Genome platform), with a simple input of the polymer repeat unit. Such an approach significantly speeds up the targeted discovery of optimal polymers that satisfy desired properties. Second, golden temperature-dependent  $E_{bd}$  data with high fidelity and its

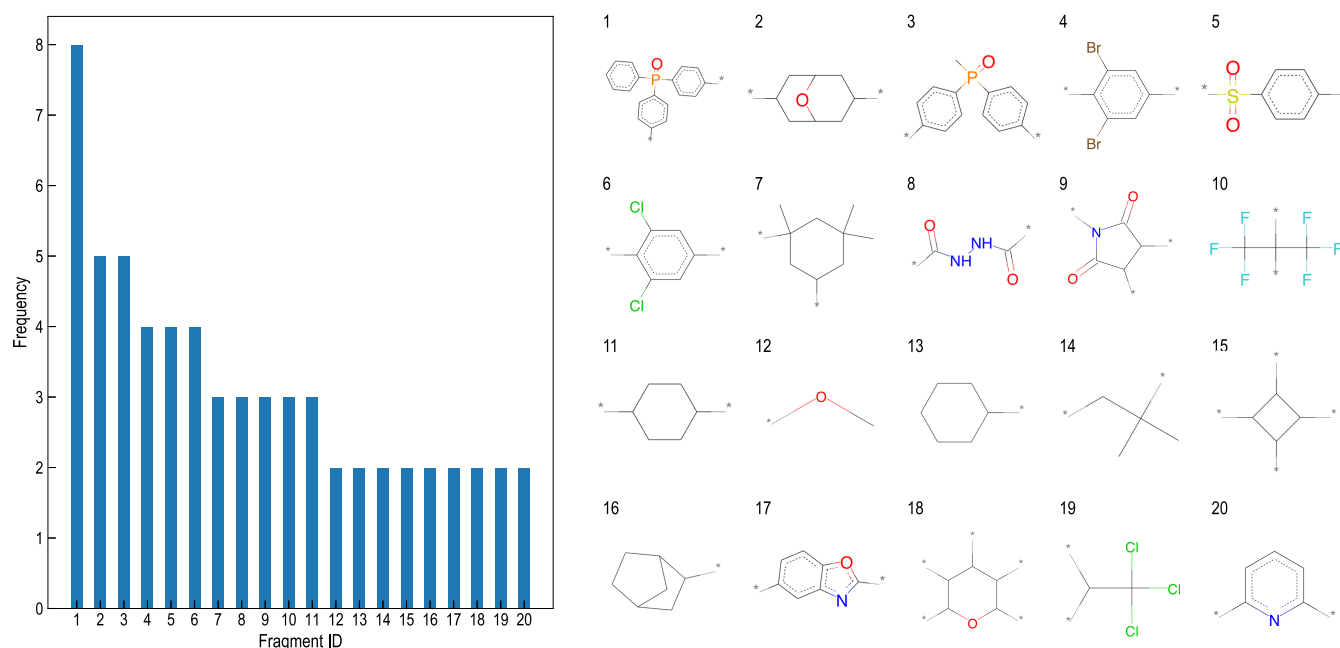


**Figure 5.** Frequency of top 20 constituting fragments of 101 polymer candidates from stage 4 in Figure 3c, together with their chemical structures.

correlations with key proxies have been provided, which benefits further  $E_{bd}$  mechanism study in electrical and electronic domains. Third, the developed protocol is extendable for other polymer applications with specific screening strategies.

There are remaining challenges for future optimization. For example, guided by the statistical analysis of correlations for key factors, a deeper mechanism study is critical. Microscopic charge dynamics and macroscopic conduction behavior under electric field extremes can provide more physical insights into the breakdown mechanism and its temperature dependence. Furthermore, it is essential to investigate the influence of morphological characteristics (such as crystalline structure and chain orientation) on breakdown strength. Another future study will be the validation of more representative polymer candidates to demonstrate the findings.

## ASSOCIATED CONTENT

### Supporting Information

The Supporting Information is available free of charge at <https://pubs.acs.org/doi/10.1021/acsami.1c11885>.

Polymer information; photograph of the experimental setup; correlations between breakdown strength and five properties; property heatmap of ML predicted band gap, electron charge injection barriers, and cohesive energy density; breakdown strength of the PVK polymer for validation (PDF)

## AUTHOR INFORMATION

### Corresponding Authors

**Rampi Ramprasad** – School of Materials Science and Engineering, Georgia Institute of Technology, Atlanta, Georgia 30332, United States; [orcid.org/0000-0003-4630-1565](https://orcid.org/0000-0003-4630-1565); Email: [rampi.ramprasad@mse.gatech.edu](mailto:rampi.ramprasad@mse.gatech.edu)

**Yang Cao** – Electrical Insulation Research Center, University of Connecticut, Storrs, Connecticut 06269, United States; [orcid.org/0000-0001-7034-2792](https://orcid.org/0000-0001-7034-2792); Email: [yang.cao@uconn.edu](mailto:yang.cao@uconn.edu)

## Authors

**Chao Wu** – Electrical Insulation Research Center, University of Connecticut, Storrs, Connecticut 06269, United States; [orcid.org/0000-0002-4565-8231](https://orcid.org/0000-0002-4565-8231)

**Lihua Chen** – School of Materials Science and Engineering, Georgia Institute of Technology, Atlanta, Georgia 30332, United States; [orcid.org/0000-0002-9852-8211](https://orcid.org/0000-0002-9852-8211)

**Ajinkya Deshmukh** – Institute of Materials Science, University of Connecticut, Storrs, Connecticut 06269, United States

**Deepak Kamal** – School of Materials Science and Engineering, Georgia Institute of Technology, Atlanta, Georgia 30332, United States; [orcid.org/0000-0003-1943-7774](https://orcid.org/0000-0003-1943-7774)

**Zongze Li** – Electrical Insulation Research Center, University of Connecticut, Storrs, Connecticut 06269, United States

**Pranav Shetty** – School of Computational Science and Engineering, Georgia Institute of Technology, Atlanta, Georgia 30332, United States; [orcid.org/0000-0003-2015-9556](https://orcid.org/0000-0003-2015-9556)

**Jierui Zhou** – Electrical Insulation Research Center, University of Connecticut, Storrs, Connecticut 06269, United States

**Harikrishna Sahu** – School of Materials Science and Engineering, Georgia Institute of Technology, Atlanta, Georgia 30332, United States; [orcid.org/0000-0001-5458-9488](https://orcid.org/0000-0001-5458-9488)

**Huan Tran** – School of Materials Science and Engineering, Georgia Institute of Technology, Atlanta, Georgia 30332, United States; [orcid.org/0000-0002-8093-9426](https://orcid.org/0000-0002-8093-9426)

**Gregory Sotzing** – Institute of Materials Science, University of Connecticut, Storrs, Connecticut 06269, United States

Complete contact information is available at: <https://pubs.acs.org/doi/10.1021/acsami.1c11885>

### Author Contributions

†C.W. and L.C. contributed equally to this work.

### Notes

The authors declare no competing financial interest.

## ACKNOWLEDGMENTS

This work is supported by the Office of Naval Research through N00014-17-1-2656, a Multi-University Research Initiative (MURI) grant. Chao Wu and Yang Cao would like to thank JoAnne Ronzello for the help in breakdown measurements.

## REFERENCES

- (1) Pourrahimi, A. M.; Olsson, R. T.; Hedenqvist, M. S. The Role of Interfaces in Polyethylene/Metal-Oxide Nanocomposites for Ultra-high-Voltage Insulating Materials. *Adv. Mater.* **2018**, *30*, 1703624.
- (2) Khanchaitip, P.; Han, K.; Gadinski, M. R.; Li, Q.; Wang, Q. Ferroelectric Polymer Networks with High Energy Density and Improved Discharged Efficiency for Dielectric Energy Storage. *Nat. Commun.* **2013**, *4*, 1–7.
- (3) Wu, C.; Deshmukh, A. A.; Li, Z.; Chen, L.; Alamri, A.; Wang, Y.; Ramprasad, R.; Sotzing, G. A.; Cao, Y. Flexible Temperature-Invariant Polymer Dielectrics with Large Bandgap. *Adv. Mater.* **2020**, *32*, 2000499.
- (4) Li, Q.; Chen, L.; Gadinski, M. R.; Zhang, S.; Zhang, G.; Li, H.; Iagodkine, E.; Haque, A.; Chen, L.; Jackson, T. N.; Wang, Q. Flexible High-Temperature Dielectric Materials from Polymer Nanocomposites. *Nature* **2015**, *523*, 576.
- (5) Azizi, A.; Gadinski, M. R.; Li, Q.; AlSaud, M. A.; Wang, J.; Wang, Y.; Wang, B.; Liu, F.; Chen, L.; Alem, N.; Wang, Q. High-Performance Polymers Sandwiched with Chemical Vapor Deposited Hexagonal Boron Nitrides as Scalable High-Temperature Dielectric Materials. *Adv. Mater.* **2017**, *29*, 1701864.
- (6) Sharma, V.; Wang, C.; Lorenzini, R. G.; Ma, R.; Zhu, Q.; Sinkovits, D. W.; Pilania, G.; Oganov, A. R.; Kumar, S.; Sotzing, G. A.; et al. Rational Design of All Organic Polymer Dielectrics. *Nat. Commun.* **2014**, *5*, 4845.
- (7) Mannodi-Kanakkithodi, A.; Treich, G.; Huan, T. D.; Ma, R.; Tefferi, M.; Cao, Y.; Sotzing, G.; Ramprasad, R. Rational Co-design of Polymer Dielectrics for Energy Storage. *Adv. Mater.* **2016**, *28*, 6277–6291.
- (8) Mannodi-Kanakkithodi, A.; Pilania, G.; Huan, T. D.; Lookman, T.; Ramprasad, R. Machine Learning Strategy for the Accelerated Design of Polymer Dielectrics. *Sci. Rep.* **2016**, *6*, 20952.
- (9) Kamal, D.; Wang, Y.; Tran, H. D.; Chen, L.; Li, Z.; Wu, C.; Nasreen, S.; Cao, Y.; Ramprasad, R. Computable Bulk and Interfacial Electronic Structure Features as Proxies for Dielectric Breakdown of Polymers. *ACS Appl. Mater. Interfaces* **2020**, *12*, 37182–37187.
- (10) Chen, L.; Batra, R.; Ranganathan, R.; Sotzing, G.; Cao, Y.; Ramprasad, R. Electronic Structure of Polymer Dielectrics: The Role of Chemical and Morphological Complexity. *Chem. Mater.* **2018**, *30*, 7699–7706.
- (11) Li, H.; Gadinski, M. R.; Huang, Y.; Ren, L.; Zhou, Y.; Ai, D.; Han, Z.; Yao, B.; Wang, Q. Crosslinked Fluoropolymers Exhibiting Superior High-Temperature Energy Density and Charge-Discharge Efficiency. *Energy Environ. Sci.* **2020**, *13*, 1279–1286.
- (12) Mannodi-Kanakkithodi, A.; Treich, G. M.; Huan, T. D.; Ma, R.; Tefferi, M.; Cao, Y.; Sotzing, G. A.; Ramprasad, R. Rational Co-Design of Polymer Dielectrics for Energy Storage. *Adv. Mater.* **2016**, *28*, 6277–6291.
- (13) Li, Z.; Treich, G. M.; Tefferi, M.; Wu, C.; Nasreen, S.; Scheirey, S. K.; Ramprasad, R.; Sotzing, G. A.; Cao, Y. High Energy Density and High Efficiency All-Organic Polymers with Enhanced Dipolar Polarization. *J. Mater. Chem. A* **2019**, *7*, 15026–15030.
- (14) Doan Tran, H.; Kim, C.; Chen, L.; Chandrasekaran, A.; Batra, R.; Venkatram, S.; Kamal, D.; Lightstone, J. P.; Gurnani, R.; Shetty, P.; et al. Machine-Learning Predictions of Polymer Properties with Polymer Genome. *J. Appl. Phys.* **2020**, *128*, 171104.
- (15) Kim, C.; Chandrasekaran, A.; Huan, T. D.; Das, D.; Ramprasad, R. Polymer Genome: A Data-Powered Polymer Informatics Platform for Property Predictions. *J. Phys. Chem. C* **2018**, *122*, 17575–17585.
- (16) Mark, J. *Polymer Data Handbook*; Oxford University Press, 1999.
- (17) Otsuka, S.; Kuwajima, I.; Hosoya, J.; Xu, Y.; Yamazaki, M. PoLyInfo: Polymer Database for Polymeric Materials Design. *2011 International Conference on Emerging Intelligent Data and Web Technologies*; IEEE: Piscataway, NJ, 2011; pp 22–29.
- (18) Huan, T. D.; Ramprasad, R. Polymer Structure Predictions from First Principles. *J. Phys. Chem. Lett.* **2020**, *11*, 5823–5829.
- (19) Dissado, L. A.; Fothergill, J. C. *Electrical Degradation and Breakdown in Polymers*; IET: London, 1992.
- (20) Holz, J.; Schulte, F. *Solid Surface Physics*; Hohler, G., Ed.; Springer, 1979.
- (21) Fowler, R. H. The Analysis of Photoelectric Sensitivity Curves for Clean Metals at Various Temperatures. *Phys. Rev.* **1931**, *38*, 45–56.
- (22) Chen, L.; Kim, C.; Batra, R.; Lightstone, J. P.; Wu, C.; Li, Z.; Deshmukh, A. A.; Wang, Y.; Tran, H. D.; Vashishta, P.; et al. Frequency-Dependent Dielectric Constant Prediction of Polymers Using Machine Learning. *NPJ. Comput. Mater.* **2020**, *6*, 1–9.
- (23) Wu, C.; Li, Z.; Treich, G. M.; Tefferi, M.; Casalini, R.; Ramprasad, R.; Sotzing, G. A.; Cao, Y. Dipole-Relaxation Dynamics in A Modified Polythiourea with High Dielectric Constant for Energy Storage Applications. *Appl. Phys. Lett.* **2019**, *115*, 163901.
- (24) Chen, L.; Pilania, G.; Batra, R.; Huan, T. D.; Kim, C.; Kuenneth, C.; Ramprasad, R. Polymer Informatics: Current Status and Critical Next Steps. *Mater. Sci. Eng., R* **2021**, *144*, 100595.
- (25) Ramprasad, R.; Batra, R.; Pilania, G.; Mannodi-Kanakkithodi, A.; Kim, C. Machine Learning in Materials Informatics: Recent Applications and Prospects. *NPJ. Comput. Mater.* **2017**, *3*, 54.
- (26) Wu, S.; Kondo, Y.; Kakimoto, M.; Yang, B.; Yamada, H.; Kuwajima, I.; Lambard, G.; Hongo, K.; Xu, Y.; Shiomi, J.; Schick, C.; Morikawa, J.; Yoshida, R. Machine-Learning-Assisted Discovery of Polymers with High Thermal Conductivity Using A Molecular Design Algorithm. *NPJ. Comput. Mater.* **2019**, *5*, 1–11.
- (27) Barnett, J. W.; Bilchak, C. R.; Wang, Y.; Benicewicz, B. C.; Murdock, L. A.; Bereau, T.; Kumar, S. K. Designing Exceptional Gas-Separation Polymer Membranes Using Machine Learning. *Sci. Adv.* **2020**, *6*, No. eaaz4301.
- (28) Shen, Z.-H.; Wang, J.-J.; Jiang, J.-Y.; Huang, S. X.; Lin, Y.-H.; Nan, C.-W.; Chen, L.-Q.; Shen, Y. Phase-Field Modeling and Machine Learning of Electric-Thermal-Mechanical Breakdown of Polymer-Based Dielectrics. *Nat. Commun.* **2019**, *10*, 1–10.
- (29) Bicerano, J. *Prediction of Polymer Properties*; CRC Press: Boca Raton, FL, 2002.
- (30) Huan, T. D.; Mannodi-Kanakkithodi, A.; Kim, C.; Sharma, V.; Pilania, G.; Ramprasad, R. A Polymer Dataset for Accelerated Property Prediction and Design. *Sci. Data* **2016**, *3*, 160012.
- (31) Tan, D.; Zhang, L.; Chen, Q.; Irwin, P. High-Temperature Capacitor Polymer Films. *J. Electron. Mater.* **2014**, *43*, 4569–4575.
- (32) Tan, Q.; Irwin, P.; Cao, Y. Advanced Dielectrics for Capacitors. *IEEJ. Trans. FM* **2006**, *126*, 1153–1159.
- (33) Yuan, C.; Zhou, Y.; Zhu, Y.; Liang, J.; Wang, S.; Peng, S.; Li, Y.; Cheng, S.; Yang, M.; Hu, J.; et al. Polymer/Molecular Semiconductor All-Organic Composites for High-Temperature Dielectric Energy Storage. *Nat. Commun.* **2020**, *11*, 1–8.
- (34) Banerjee, T.; Lipscomb, G. G. Direct Measurement of the Carbon Dioxide-Induced Glass Transition Depression in A Family of Substituted Polycarbonates. *J. Appl. Polym. Sci.* **1998**, *68*, 1441–1449.
- (35) Scorțanu, E.; Nicolaescu, I.; Caraculacu, A. A.; Caraculacu, G. Dibenzylic Structure on the Macromolecular Chain. XII. Polyureas: Structure-Property Relationships. *Polym. Int.* **2000**, *49*, 881–887.
- (36) Rangaswamy, K.; Narasimham, A.; Sobhanadri, J. Electrical DC Conductivity of Some Aromatic Polyamides. *Indian J. Pure Appl. Phys.* **1994**, *32*, 489–493.
- (37) Liaw, D.-J.; Chang, P. Synthesis and Characterization of Aromatic and Brominated Aromatic Polycarbonates by Two-Phase Phase-Transfer-Catalyzed Polycondensation of Bisphenols with Trichloromethyl Chloroformate. *J. Appl. Polym. Sci.* **1997**, *63*, 195–204.
- (38) Shell Chemical Corporation. *Ind. Eng. Chem.* **1959**, *51*, 20A.



(39) RDKit, Open Source Toolkit for Cheminformatics; <http://www.rdkit.org/>.